

Corrosion protection of mild steel by environment friendly Polypyrrole/Gum Acacia Composite Coatings

Gazala Ruhi¹, Pradeep Sambyal², Hema Bhandari¹, Haritma Chopra¹ and Sundeep K. Dhawan^{2*}

¹ Department of Chemistry, Maitreyi College, University of Delhi, New Delhi 110021, India

² Polymeric & Soft Materials Section, CSIR-National Physical Laboratory, Dr. K.S. Krishnan Marg, New Delhi 110012, India

*Corresponding author.

DOI: 10.5185/amlett.2018.7007

www.vbripress.com/aml

Abstract

In a novel approach, Polypyrrole/Gum Acacia composites (PPy/GA) were synthesized by in-situ oxidative polymerization of pyrrole on the Gum Acacia (GA) surface by using FeCl_3 as oxidant. The ¹H NMR and FTIR confirms the presence of peaks of Polypyrrole and Gum Acacia in the composite. The microstructural analysis of the composite reveals uniform layer of Polypyrrole on the surface of GA particles. The X-ray Diffraction pattern reveals the amorphous nature of the composite. Powder coating technique was used to design the composite coatings. The electrochemical studies like Open Circuit Potential (OCP) variation with time, Potentiodynamic Polarization and Electrochemical Impedance Spectroscopy (EIS) were conducted in 3.5% NaCl solution to evaluate the corrosion resistance of the coatings. The composite coatings demonstrated superior corrosion resistance in salt spray fog of 5.0% NaCl (under accelerated test conditions in salt spray chamber). The synergistic combination of the corrosion inhibition properties of Gum Acacia and the redox properties of Polypyrrole is the reason for the occurrence of high corrosion resistance of the composite coatings. The present coating composition has shown excellent corrosion resistance and can be a potential coating formulation for mild steel substrate used in various applications under saline conditions. Copyright © 2018 VBRI Press.

Keywords: Gum acacia, polypyrrole, EIS, potentiodynamic polarization.

Introduction

Mild steel is a widely used engineering material with extensive usage in a wide range of industrial applications. This steel is less expensive, has superior mechanical strength and good machinability. However, mild steel is very vulnerable towards corrosion. The rate of corrosion further accelerates many folds in sea water environment because of the presence of diffusive chloride ions. Among the various methods of corrosion protection of mild steel, application of corrosion resistant coatings is one of the efficient methods. The coatings act as a barrier and isolate the metal surface from the corrosive electrolyte [1-4]. Chromate conversion coatings have superior corrosion protection properties with an ability to replenish the mechanical integrity of the coatings when subjected to mechanical damage. However, the toxicity and carcinogenic property of chromate ions have eliminated its use in coating applications. Further, organic coatings also play an important role for the corrosion protection of metallic substrates. This is because of their efficient barrier properties and good mechanical integrity. Among various organic coatings, epoxy coatings/paints are frequently used for corrosion protection purpose in marine environment [5, 6]. These coatings have good

adhesion to the metal surface because of the presence of polar groups in the resin. The corrosion protection of epoxy coatings depends on the molecular weight of the resin, cross linking density of the resin, concentration of curing agent etc. Epoxy coatings with high cross-linking density exhibit excellent anticorrosion behaviour. It makes difficult for aggressive ions to penetrate through the coating [7]. However, mechanical abrasion/damage severely compromises the corrosion protection efficiency of the epoxy coatings. The defects create pathways for the diffusion of water, oxygen, and corrosive species onto the metallic substrate and resulting in the localized corrosion [8]. In order to improve the corrosion resistance property of the coatings, the epoxy resin is reinforced with various fillers [9, 10]. In addition to this, natural corrosion inhibitors/organic polymers/nano particles can be incorporated in the polymer matrix to improve the overall properties of the coating.

Plants extracts have shown splendid applications in various fields because of their eco friendly nature. Some plant extracts are also rich source of environment friendly corrosion inhibitors. These inhibitors form a protective film on to the metal surface separating the metal from the corrosive environment [11-17]. The inhibitors are easily available green compounds that are biocompatible, bio-

degradable and less expensive. Gum Acacia (GA) is a natural polymer mainly consists of high molecular weight polysaccharides and contains high concentrations of calcium, magnesium and potassium salts. Gum Acacia (GA) is a green alternative for corrosion protection of mild steel in both acidic and alkaline medium [18-22]. It is cost effective, environment friendly and free from toxic by products [23]. Literature has shown that there exist interaction between Gum Acacia and steel surface [24]. The coordination type bonding is assumed to occur between the ferrous ions and the oxygen atoms present in the backbone of the polymer. However, most of the studies on the corrosion inhibition of Gum Acacia are conducted under ambient conditions and the achieved corrosion protection efficiency is very low.

Intrinsically conducting polymers (ICPs) like Polyaniline, Polypyrrole etc. are conjugated systems that are prevalently discussed as useful corrosion protection materials for active metals such as mild steel, aluminium, zinc etc. [25-32]. These polymers exhibit redox behaviour and provide anodic protection to the underlying metal by shifting the potential of the metal in passive region. DeBerry first reported that stainless steel coated with Polyaniline coatings kept the potential of the steel in passive region for relatively longer period in sulphuric acid solution [33]. Reports showed that the Polypyrrole and Polyaniline exhibit self healing properties by which they can replenish the integrity of the coatings at the sites of defects and pores [34]. Our previous works demonstrated Polypyrrole based composite coatings with superior corrosion resistance properties [35-37]. The reported works have studied how the Polypyrrole composites improved the corrosion resistance of epoxy coatings under extremely corrosive environments. There are constant efforts to designed Conducting polymer based composite coatings to exploit the synergy of the constituents and to design coatings with excellent barrier properties even in prolong periods of immersion in corrosive electrolyte.

In view of the above, the present investigation focuses on the synergistic interaction between Polypyrrole and Gum Acacia to design polymer composites with superior corrosion resistance properties. The synthesized composites will exhibit the corrosion inhibition property of Gum Acacia and redox behaviour of Polypyrrole. As per our knowledge, no work has been carried so far to synthesize Polypyrrole/Gum Acacia composites for corrosion protection purpose. In this work, we herein propose the synthesis of a novel Polypyrrole/Gum Acacia (Ppy/GA) composite by in situ emulsion polymerization of Pyrrole monomer. Coatings were developed by blending the composites in epoxy powder coating formulations, followed by spraying and curing on the metal surface. The electrochemical behaviour of the coatings was evaluated by OCP vs time, Tafel polarization and electrochemical impedance spectroscopy (EIS) in 3.5% NaCl solution. Corrosion resistance under accelerated test conditions are carried out in salt spray fog of 5.0% NaCl with a relative humidity of 65%. The

tabulated comparison of the reported work with the previously reported literature is shown in **Table 1**.

Present work is expected to produce coating formulations that will significantly improve the corrosion resistance of commercially available epoxy coatings. The synthesized composites are environment friendly and have almost no residual impact on environment. The coatings are developed using powder coating technique, which is environmentally viable technique with no VOC (volatile organic compound) emission. Additionally, the proposed work will pave the way to design different coating formulations by combining different plant based corrosion inhibitors with the conjugated polymers. The principle of this work is to exploit the synergistic combination of the properties of natural (plant based) inhibitors and conjugated polymers.

Reported Work	Previously Reported Literature
The corrosion resistance of plant based inhibitor (Gum Acacia) and organic Conjugated polymer (Polypyrrole) is combined to form composite coatings, in the reported work. The reported composite coatings have exhibited excellent corrosion protection to the substrate for prolong period of immersion.	Previous literature show designing of Polypyrrole based composite coatings for corrosion protection of metals [38-40], however Polypyrrole/Gum Acacia composite coatings are not reported. Previous literature reported the corrosion studies of coatings for a short exposure time [39, 41]. The detailed discussion on the corrosion kinetics with the lapse of time is also not mentioned.
Extensive electrochemical data has been provided in the reported work to study the behaviour of the coating during the exposure period of 30 days. The reported composite coating withstand highly corrosive conditions of salt spray fog (ASTM B117) and has shown superior corrosion resistance.	Previous literature show fewer days of exposure of Polypyrrole based composite coatings under salt spray fog [42, 43] and hence a longer duration corrosion test under highly corrosive conditions is needed.

Experimental

Chemicals and materials

For synthesis, Pyrrole (Acros Organics, 99%) was distilled and stored under nitrogen at 4 °C temperature, prior to use. Sodium lauryl sulphate (SLS) and Ferric chloride (FeCl₃) were purchased from Merck Chemicals.

Gum Acacia (GA) was purchased from Qualigens fine chemicals. The steel sheet of composition, C= 0.18%, Mn= 0.5%, P= 0.04%, S= 0.06% and Fe = balance was cut to a dimension of 10mm x 40mm x 2mm for corrosion studies and 150mm x 100 mm x 2mm for salt spray tests. The cut specimens were polished metallographically by grinding them with emery papers of 120, 600 and 800 grit size to attain a smooth finish. Thereafter, the steel specimens were cleaned ultrasonically in ethanol and distill water.

Synthesis of Polypyrrole/Gum Acacia (PPy/GA) composites

Polypyrrole/Gum Acacia (PPy/GA) composites were synthesized by in-situ chemical oxidative emulsion polymerization of Pyrrole in presence of Gum Acacia (GA). In the polymerization process, Ferric chloride is used as an oxidant and Sodium lauryl sulphate as surfactant. Firstly, distillation of the monomer (Pyrrole) is carried out in order to remove the impurities present in it. Gum Acacia (GA) powder is taken in a reaction vessel and Pyrrole is added to it with continuous stirring. The mixing process is carried out at 50 °C for proper encapsulation of the monomer on the gum acacia powder. The Gum acacia (GA) is kept to be 25.0 wt% of the monomer (Pyrrole). The continuous addition of Pyrrole results into the formation of slurry, which is added slowly to distilled water containing Sodium lauryl sulphate (SLS). The suspension was stirred vigorously for proper mixing and homogenization. This was followed by drop wise addition of Ferric chloride solution. The molar ratio of Pyrrole:SLS:FeCl₃ is 0.1:0.01:0.1. The polymerization of Pyrrole starts immediately after the addition of Ferric chloride solution. The appearance of black color powder showed the start of polymerization of Pyrrole. The composite was retrieved by filtering with G 4 Buchner filtration funnel. The powder was washed with deionised water (to remove oxidant and oligomers) and dried in a vacuum oven at 60 °C.

Development of powder coating

The epoxy powder coating formulation having composition: resin {epoxy (bisphenol A+polyester) (70%), Flow agent (D-88) (2.3%), degassing agent (benzoin) (0.7%), fillers (TiO₂ and BaSO₄) (27%) is used in the present study. The synthesized polymer composites (PPy/GA) were blended with epoxy in various wt% loadings (1.0, 2.0, 3.0 and 4.0) using a laboratory ball mill. The homogeneously dispersed PPy/GA composites in epoxy are the final powder coating formulations. The powder coating formulations were applied on mild steel specimens using an electrostatic spray gun held at 67.4 KV potential with respect to the substrate (grounded). The powder coated mild steel specimens were cured in oven at 165 °C for 30 minutes. The coated specimens were designated as follows, uncoated steel (BS), epoxy coated steel (EC), epoxy with different wt% loading of Polypyrrole/Gum Acacia (PPy/GA) composite

coatings (PA1 for 1.0 %), (PA2 for 2.0 %), (PA3 for 3.0 %) and (PA4 for 4.0 %) in text, figures and tables.

Characterization

Characterization of Polypyrrole/Gum Acacia (PPy/GA) composite

¹HNMR spectra of Polypyrrole and Polypyrrole/Gum Acacia (PPy/GA) were recorded (DMSO-d₆ as solvent) using high resolution spectrometer (NMR; Bruker 300 MHz, Germany) having tetramethylsilane (TMS) as an internal standard. The chemical composition of the polymer composite (PPy/GA) was analyzed using Fourier Transform Infrared (FTIR) spectroscopy (Model- Nicolet 5700) in the spectral range of 4000-600 cm⁻¹. The spectrum was recorded by analyzing powdered composite samples in KBr pellets. Spectrum was collected by performing 32 scans with a resolution of 4 cm⁻¹.

Bruker D8 Advanced diffractometer with CuK α radiation (λ = 1.54 Å) in the scattering range (2 θ) of 10°–80°, was used for the XRD analysis of the polymer composites. Microstructural analysis of the polymer composites was studied using Scanning Electron Microscope (JEOL- JSM-6360A) and Transmission Electron Microscope (Tecnai TMG F30, FEI). The surface topography of the coatings after 30 days of immersion in 3.5% NaCl solution was also viewed under SEM. The elemental composition of the coated surface was observed by energy-dispersive X-ray spectrometry (EDS) attached with the SEM.

Electrochemical measurements

The corrosion resistance of the coated/uncoated steel specimens was measured by studying the variation of Open Circuit Potential (OCP) with time, Potentiodynamic Polarization (Tafel plots) and Electrochemical Impedance Spectroscopy (EIS) in 3.5% NaCl solution open to air at room temperature (30 \pm 2 °C). The 3.5% NaCl solution was prepared using analytical grade reagents and distilled water. An electrochemical workstation (Autolab Potentiostat/ Galvanostat, PGSTAT100) was used to carry out the electrochemical measurements. The measurements were examined using a standard three electrode electrochemical cell with a Pt rod as counter electrode, Ag/AgCl as reference electrode and each coated/uncoated steel specimen (1 cm² area exposed) as working electrode. All the electrode potentials are measured with reference to Ag/AgCl. Prior to the electrochemical tests, the specimens were stabilized in 3.5% NaCl solution for 30 minutes. Tafel plots were recorded by carrying out potentiodynamic polarization at a constant scan rate of 1mV/sec by sweeping the potential between \pm 250 mV vs Ag/AgCl from E_{corr}. Various electrochemical parameters like corrosion potential (E_{corr}), corrosion current density (i_{corr}), corrosion rate (C.R., mm/year) were derived by extrapolating the anodic and cathodic curves of the Tafel plots. EIS measurements were performed to derive the values different impedance parameters like pore resistance (R_{pore}) and coating capacitance (C_c), Warburg

impedance (W) by fitting suitable equivalent circuits. The measurements were carried out at open circuit potential with 10 mV amplitude of sine potential signal in the applied frequency range of 100 KHz to 0.1 Hz. Salt spray tests were conducted as per ASTM B117 method to estimate the corrosion tolerance of the coated steel panels under accelerated test conditions. For this, the coated steel panels were exposed to salt spray fog containing 5.0 % NaCl solution for a period of 120 days.

Results and discussion

Nuclear Magnetic Resonance Spectroscopy (^1H NMR)

The ^1H NMR spectra of Polypyrrole and Polypyrrole/Gum Acacia (PPy/GA) composite in DMSO- d_6 solvent are shown in Fig. S1 a and b, respectively (Supplementary information). For Polypyrrole, a characteristic signal at 7.0- 7.4 ppm is assigned to the aromatic protons present in PPy chain and the signal at around 8.2 ppm indicates the N-H protons of polypyrrole ring. Gum Acacia shows characteristic signals at 2.6 ppm due to acid protons present in the sugar moiety and a peak at around 3.3 ppm attributing to the sugar protons [44-45]. The PPy/GA composite (Fig. S1b) exhibits the characteristic signals of GA molecules at 2.46 ppm (corresponding to the acid protons present in the sugar moiety of Gum Acacia (GA) molecule) and at 3.48 ppm (indicating the sugar protons present in GA molecules). However, the signals are slightly shifted as compared to the neat GA molecules. The shifting of the signals is due to the interaction between Polypyrrole chain and the GA molecules. The characteristic signals of aromatic protons and N-H protons of Polypyrrole are also observed to be shifted to 7.2- 7.4 ppm and 8.7 ppm, respectively. Shifting of these signals also gives strong indication of the interaction between PPy and GA during polymerization. Further, ^1H NMR spectrum of PPy/GA composite shows two signals at $\delta = 1.0$ ppm and 0.9 ppm which indicates protons attached to the methylene ($-\text{CH}_2$) and methyl groups ($-\text{CH}_3$) of sodium lauryl sulphate unit respectively at PPy/GA composite. Therefore, ^1H NMR spectra of PPy/GA composite confirms the interaction of GA molecules with Polypyrrole chain in the presence of Sodium Lauryl Sulphate.

FTIR and XRD studies

The FTIR spectra of Gum Acacia (GA) and Polypyrrole/Gum Acacia (PPy/GA) composite is shown in Fig. S2 (Supplementary information). The FTIR spectrum of GA shows a broad absorption band at a spectral range of 3872-3000 cm^{-1} , assigning to the stretching vibration of O-H bond. The occurrence of a low intensity peak at 2923 cm^{-1} is due to the stretching vibration of C-H bonds. Appearance of an appreciably high intensity peak at 1635 cm^{-1} is due to the stretching vibration of C=O bonds of carboxylate groups associated with the GA molecule [46]. The peaks of medium intensity at 1425 and 1067 cm^{-1} are assigned to the stretching vibration of C-O bonds. Further, appearance of

a weak absorption band at 900-500 cm^{-1} is assigned to the symmetrical and asymmetrical ring breathing vibration of C-C-O, C-O-C bonds [47]. The FTIR spectrum of PPy/GA exhibits the characteristic peaks of polypyrrole. The major FTIR peaks are located at 1554 cm^{-1} (typical pyrrole ring vibration) [48], 1474 cm^{-1} ($=\text{CH}$ in plane vibrations), 771 cm^{-1} ($=\text{CH}$ out of plane vibrations) [49-51], 1038 cm^{-1} (N-H in plane deformation absorption of polypyrrole), 1186 cm^{-1} (C-N stretching) [52]. In the composite the peaks of Gum Acacia is observed to be superimposed with the Polypyrrole. The formation of a uniform layer of polypyrrole on the surface of acacia during the polymerization could be the other reason for the suppression of the FTIR peaks of Gum Acacia (GA) in the composite. Fig. S2b illustrates the X-ray diffraction patterns obtained for Gum Acacia (GA) and Polypyrrole/Gum Acacia (PPy/GA) composite. The XRD patterns show the amorphous nature of GA and PPy/GA composite. For GA, XRD peak with the peak maxima is observed at $2\theta = 19.72^\circ$ (θ is the angle of incidence). However, the peak maxima shifted slightly towards higher 2θ value (21.96°) for the PPy/GA composite. The shifting of the peak maxima towards higher 2θ values is basically due to the change in the composition of the material.

Microstructural analysis

The SEM micrograph showing the particle morphology of Gum Acacia (GA) is shown in Fig. S3a-e (supplementary information). The GA particles are found to have smooth surface appearance. However, the shape of the particles is irregular (Fig. S3a). The particles exhibit a wide size distribution and are basically sub micron size particles. However, interesting microstructural features are noticed for Polypyrrole/Gum Acacia (PPy/GA) composite (Fig. S3b). The surface of the acacia particles are found to be uniformly covered with small spherical polypyrrole particles. The high magnification image (Fig. S3c) exhibits the morphology of the polypyrrole on Gum Acacia surface. The TEM micrograph of Polypyrrole/Gum Acacia (PPy/GA) composite is shown in Fig. S3d. The micrograph reveals the distribution of acacia particles in the polymer matrix. The EDS spectrum of PPy/GA composite is shown in Fig. S3e. The spectrum exhibits the presence of elements like Carbon (64.1%), Nitrogen (0.5%), Oxygen (25.4%) and Sulphur (9.9%) in the composite.

Electrochemical studies

Open Circuit Potential (OCP) with time

The Open Circuit Potential (OCP) with time curves are shown in Fig. 1. The trend of OCP variation was measured for 14400 s under freely corroding conditions. The OCP curve for uncoated steel (BS) shows a gradual decrease of potential with the immersion time. The gradual decrease of potential is basically due to the occurrence of uncontrolled corrosion process on the steel surface as a result of the direct contact between the metal and the

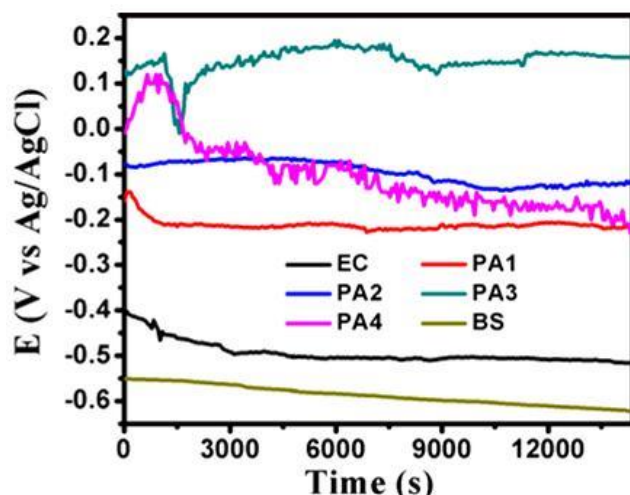


Fig. 1. The OCP vs time curves for uncoated steel (BS), epoxy coating (EC) and epoxy coatings with 1.0 wt% (PA1), 2.0 wt% (PA2), 3.0 wt% (PA3), 4.0 wt% (PA4) loading of Polypyrrole/Gum Acacia (PPy/GA) composite immersed in 3.5% NaCl solution at room temperature ($30 \pm 2^\circ\text{C}$).

electrolyte. The trend of the variation of OCP for epoxy coating (EC) exhibits the decrease of potential in the first few minutes of immersion. However, the potential became almost stable with the passage of immersion time. The trend of the OCP variation for epoxy coatings with 1.0 wt% loading of PPy/GA composite (PA1) was observed to almost similar to that of epoxy coating. A negative shift of potential is noticed in the initial period of immersion followed by attainment of a steady state value. The OCP of epoxy coating with 2.0 wt% loading of PPy/GA composite (PA2) remain almost stable throughout the immersion period revealing the equilibrium condition of the coated surface. Interesting results are noticed for epoxy coating 3.0 wt% loading of PPy/GA composite (PA3). A sudden drop of potential is noticed initially due to the rapid diffusion of electrolyte. However, the potential shifted in positively with the passage of immersion time. This positive shift of potential is basically due to the tendency of the surface film to passivate the metal surface by inhibiting the ingress of ions/electrolyte through it.

The result gives an initial idea that the PPy/GA composite present in the epoxy coating system has a tendency to block the active corrosion sites. The preliminary observation of OCP vs time illustrates the self healing mechanism of Polypyrrole and corrosion inhibition of Gum Acacia in 3.5% NaCl solution. Here it is interesting to mention that the coating systems PA1, PA2 and PA3 have demonstrated a gradual enhancement in the corrosion resistance under freely corroding conditions. However, the corrosion resistance of coating PA4 showed discouraging results. The OCP trend shows a negative shift of potential with time. This observation is supported by findings of literature which explains that the optimum corrosion protection is achieved with lower loadings of conducting polymers, whereas, porosities develop in the coatings with higher loadings of the

polymer [53-56]. However it is interesting to note that the steady state OCP values of epoxy coatings with PPy/GA composites (PA1, PA2, PA3 and PA4) are found to be significantly more positive than the neat epoxy coating (EC). The observed OCP of specimens PA1, PA2, PA3 and PA4 are 295mV, 397 mV, 668mV and 283 mV, respectively more positive than specimen EC. From the OCP trends, it can be concluded that the corrosion resistance of epoxy coatings are improved on the incorporation of PPy/GA composite. The high positive values of OCP are certainly due to the presence of an excellent coating with superior barrier properties. Additionally, it is also assumed that the coatings with PPy/GA composite have self healing property.

Tafel plots

Fig. 2 a-f compares the typical Tafel polarization curves obtained for epoxy coating (EC) and epoxy coatings with 1.0 wt% (PA1), 2.0 wt% (PA2), 3.0 wt% (PA3) and 4.0 wt% (PA4) loading of PPy/GA composite immersed in 3.5% NaCl solution at room temperature ($30 \pm 2^\circ\text{C}$) for 30 days. Table S4 (Supplementary Information) mentions the different electrochemical parameters, like corrosion potential (E_{corr}), corrosion current density (i_{corr}), corrosion rate (mm/year). The parameters are determined by extrapolating the anodic and cathodic Tafel curves using Tafel extrapolation method. **Fig. 2a** demonstrates the comparative Tafel curves after 24 hrs of immersion. The E_{corr} is observed to be almost equal (Table S4) for all the epoxy coatings (with and without PPy/GA composites). However, in comparison to neat epoxy coating (EC), the four coating formulations (PA1, PA2, PA3 and PA4) display lower corrosion current densities (i_{corr}). It is important to mention that the epoxy coating with 1.0 wt% loading of PPy/GA composite (PA1) evidenced very low current (beyond the lowest limit of the instrument), therefore, Tafel curve was not obtained for coating PA1, even after 24 hrs of immersion in 3.5% NaCl solution. Interesting Tafel curve trends are observed for the coatings after 2 days of immersion in 3.5% NaCl solution (**Fig. 2b**). The E_{corr} of neat epoxy coating (EC) shifted towards more negative potential (-654.2 mV), whereas, the corresponding E_{corr} values of specimens PA2 (-588.7 mV), PA3 (-578.4 mV) and PA4 (-687.8 mV) appeared to be shifted towards more positive potential (Table S4). In addition to this, the neat epoxy coating evidenced increase in the corrosion current density (4.6×10^{-8} A/cm²). The i_{corr} values of epoxy coatings with PPy/GA composites (Table S4) remained undisturbed. The obtained i_{corr} values clearly show the weakening of the barrier property of the neat epoxy coating with immersion time, whereas, the PPy/GA composite present in the epoxy coating passivated the metal surface by shifting the E_{corr} towards positive potential and maintaining a low value of i_{corr} . **Fig. 2 c, d, e** and **f** illustrate the comparative Tafel curves after 5 days, 10 days, 20 days and 30 days of immersion, respectively in 3.5% NaCl solution. These Tafel curves clearly demonstrate that the E_{corr} of epoxy coatings with different wt% loadings of PPy/GA composite remained

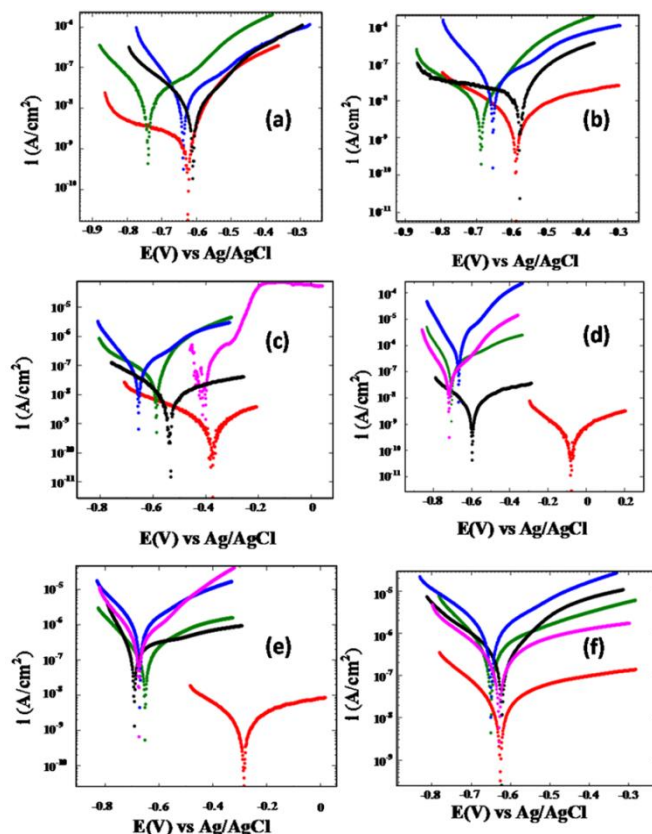


Fig. 2 The Tafel curves for epoxy coating (EC) and epoxy coatings with 1.0 wt% (PA1), 2.0 wt% (PA2), 3.0 wt% (PA3), 4.0 wt% (PA4) loading of Polypyrrole/Gum Acacia (PPy/GA) composite immersed in 3.5% NaCl solution at room temperature ($30 \pm 2^\circ\text{C}$) for (a) 24 hrs, (b) 2 days, (c) 5 days, (d) 10 days, (e) 20 days and (f) 30 days.

more positive as compared to the neat epoxy coating (Table S4), upto 30 days of immersion. In accordance with the E_{corr} , the i_{corr} values of these coatings are observed to be lower than the neat epoxy coating. Among all coatings, the epoxy coating with 2.0 wt% loading of PPy/GA composite (PA2) has demonstrated most superior corrosion resistance. The specimen PA2 showed a significant positive shift of E_{corr} with the lapse of immersion time. For PA2, the E_{corr} shifted almost 340 mV more positive after 20 days of immersion in 3.5% NaCl solution.

(Table S4). Additionally, the i_{corr} values remained very low throughout the 30 days of immersion period. It is well studied that even conventional coatings with excellent corrosion resistance and superior bonding properties degrade with the lapse of time in corrosive electrolyte. Therefore, if a coating system maintained the corrosion current low and shifts the potential of the underlying metal positively with the immersion time, the protection mechanism is other than the simple barrier type and the coating possesses a property to passivate the metal surface by recuperating the defects and pores that develop in the coating due to continuous exposure to the corrosive electrolyte. The Tafel data clearly show that the presence of Polypyrrole and Gum Acacia in epoxy coating system is responsible for occurrence of superior

corrosion inhibition even for longer period of immersion in 3.5% NaCl solution. For better understanding of the difference in corrosion resistance behaviour of the neat epoxy coating and epoxy coatings with PPy/GA composites, the corrosion surface morphologies of the two coatings, neat epoxy (EC) and epoxy with 2.0 wt% loading of PPy/GA composite (PA2) after 30 days of immersion in 3.5% NaCl solution were analysed by SEM (Fig. 3). A low magnification SEM image (Fig. 3a) shows the presence of corrosion on the epoxy coated steel surface. Small corrosion sites can be easily noticed from the micrograph. The high magnification SEM micrograph (Fig. 3b) reveals the presence of needle shaped corrosion product (hydrated iron oxide) on the surface [57-58].

It can be noticed from the micrograph that the oxide layer is porous and has irregular structure with numerous clusters of iron oxide. Therefore, it permits easy diffusion of chloride ions to the metal surface. The presence of elements like, Fe = 85.8 wt%, Na = 0.98 wt%, Cl = 0.22 wt%, C = 4.24 wt% and O = 8.41 wt% is proven by EDS profiling (Fig. 3c) of the corroded epoxy coated specimen. The presence of high wt% of Fe further confirms the presence of iron oxide layer on the surface. On the contrary, the surface morphology of epoxy coating with 2.0 wt% loading of PPy/GA composite (PA2) evidenced a homogenous and compact appearance (Fig. 3d). This featureless surface morphology at high magnification is appeared to contain nano sized plate like structures (Fig. 3e). The EDS analysis (Fig. 3f) confirmed the presence of elements, C = 43.1 wt%, O = 33.0 wt%, Si = 8.6 wt%, S = 3.9 wt%, Na = 2.8 wt%, Cl = 3.8 wt% and very less amount of Fe (1.8 wt%). The presence of very low wt% of Fe highlights that the compact layer present on the surface of PA2 is different from the regular rust layer.

The microstructural features of the coatings (EC and PA2) are in accordance with the Tafel polarization test results. During the initial period of immersion in 3.5% NaCl solution, the coatings (neat epoxy and epoxy with different wt% loadings of PPy/GA composites) showed excellent barrier property towards the penetration of electrolyte. Literature reports that the epoxy resin has polar groups present along the polymer chain that binds well with the metal surface and forms coatings with good barrier properties [59-60]. However, the coating deteriorates on prolonged immersion to the electrolyte, as the diffusive ions degrade the metal coating bond causing failure of the barrier property of the coating. Here, the epoxy coatings with PPy/GA composites maintained the superior corrosion resistance of the coatings even after prolonged exposure to chloride ions.

The synergistic effect of the corrosion inhibition properties of Polypyrrole and Gum Acacia is the basic reason of the superior corrosion resistance of the coatings. The Polypyrrole shows redox property and intercepts the electron released from the metal and utilise them to reduction of oxygen at coating/electrolyte interface. This reaction assists in the formation of a passive oxide layer at the polymer / metal interface, which shifts the corrosion

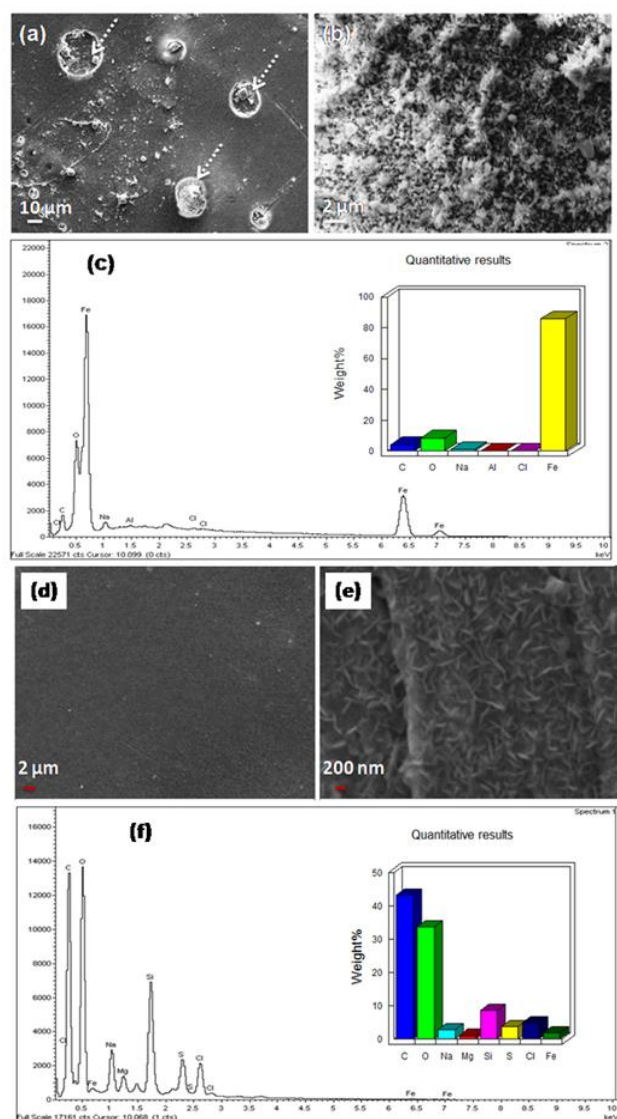


Fig. 3 (a) The surface morphology of epoxy coating (EC) after 30 days of immersion in 3.5% NaCl solution. (b) High magnification image showing needle shaped rust present on the coated surface. (c) EDS spectrum of the corroded coated surface. (d) The surface morphology of epoxy with 2.0 wt% loading of PPy/GA composite (PA2) coating after 30 days of immersion in 3.5% NaCl solution. (e) High magnification surface image showing plate like nano structures. (f) EDS spectrum of the coat.

potential of the mild steel to noble direction. Further, the Gum Acacia assists the formation of oxide layer on the metal surface. Gum Acacia is a branched complex polysaccharide having pronounced corrosion inhibition property [61–65]. It simply adsorbs on the metal surface through their oxygen and nitrogen atoms and blocks the cathodic and anodic sites. In this way, the two constituents of the composite synergistically improve the corrosion resistance of the epoxy coating system.

Electrochemical Impedance Spectroscopy (EIS)

The Nyquist curves of neat epoxy coatings (EC) and epoxy coatings with different wt% loadings of PPy / GA composites (PA1, PA2, PA3 and PA4) immersed in 3.5%

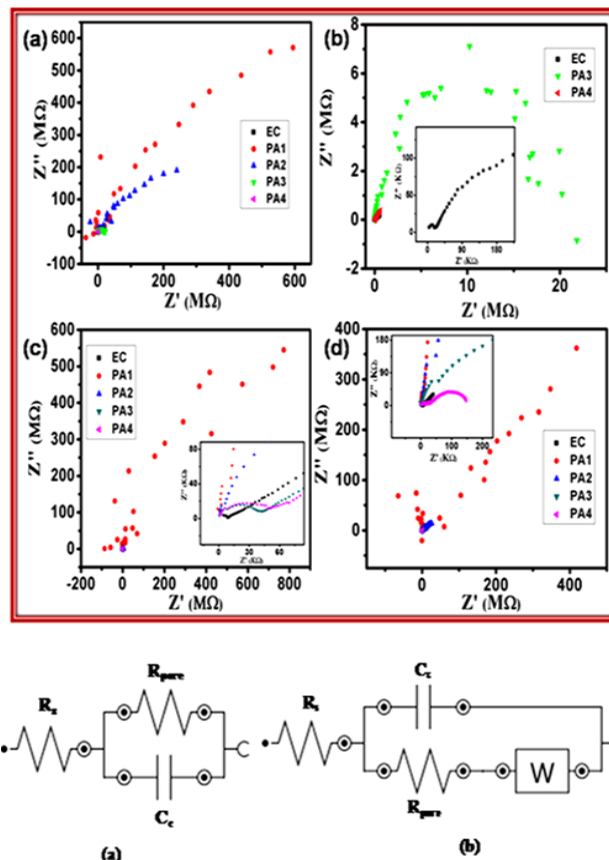


Fig. 4. Nyquist curves of epoxy coatings (EC) and epoxy coatings with 1.0 wt% (PA1), 2.0 wt% (PA2), 3.0 wt% (PA3), 4.0 wt% (PA4) loading of Polypyrrole/Gum Acacia (PPy/GA) composite after (a-b) 4 hrs, (c) 24 hrs and (d) 4 days of immersion in 3.5% NaCl solution at room temperature ($30 \pm 2^\circ\text{C}$). Electrical equivalent circuits of (a) intact coating in contact with electrolyte, (b) coatings showing diffusion of electrolyte. Here, R_e (electrolyte resistance), R_{pore} (pore resistance), C_e (coating capacitance) and W (Warburg impedance).

NaCl solution for 30 days are shown in **Fig. 4** and **5**. The corresponding Bode curves are shown in **Fig. 6**. The equivalent circuits as shown in **Fig. 4e-f** are used to extract the different EIS parameters. **Fig. 4a** and **b** illustrate the Nyquist curves of coatings after 4 hrs of immersion. From the curves, it can be noticed that all the epoxy coatings with PPy/GA composites show similar Nyquist trend, indicating the similar corrosion mechanism in the initial hrs of immersion. They exhibit capacitive arc manifesting an effective corrosion protection to the substrate. The high frequency region Nyquist curves, as shown in **Fig. 4b** reveals that the neat epoxy coating has a high frequency capacitive arc followed by a low frequency diffusion tail. The observation of diffusion tail indicates the occurrence of diffusion process at the coating/metal interface [66]. Here, the corrosion process is diffusion controlled. The presence of diffusion phenomenon makes a clear indication that the barrier property of the epoxy coating is compromised even in the initial period of immersion in 3.5% NaCl solution. A simple Randle circuit, consisting of a resistor connected in series to a parallelly connected resistor and capacitor (**Fig. 4e**) is used to fit the experimentally obtained EIS data for epoxy coatings with PPy/GA composites.

Whereas, another electrical equivalent circuit (**Fig. 4f**) having an additional circuit element i.e. Warburg impedance (W) is adopted to fit the experimentally obtained EIS data for neat epoxy coatings. **Table 2** mentions the values of EIS parameters like pore resistance (R_{pore}), coating capacitance (C_c) and Warburg impedance (W) for the coating systems. Pore resistance (R_{pore}), is the measure of electrical resistance of the coating system and signifies the performance of the surface coating, whereas, coating capacitance (C_c) is related to water uptake tendency of the coating. Warburg impedance is the diffusion impedance that indicates the occurrence of diffusion of ionic species at the coating/metal interface and the polarization is due to a combination of kinetic and diffusion processes. The Warburg impedance is related to the porosities present in the coatings, and is expressed as

$$W = \frac{\sigma}{\sqrt{\omega}}$$

Here, σ is Warburg coefficient and ω is angular frequency ($2\pi f$) at which the Warburg diffusion starts. Literature reports that the term Warburg coefficient (σ) is inversely related to the diffusion coefficient [67]. Therefore, higher the values of Warburg impedance (W) lower will be the rate of diffusion controlled corrosion reaction. The Nyquist curves for epoxy coating (EC) evidenced prevalent diffusion controlled corrosion process through the coating (**Fig. 4, 5**). The values of Warburg impedance remained very low and further reduced with the lapse of immersion time

(Table S5, Supplementary Information). Accordingly, the R_{pore} remained very low, signifying the low resistance of the surface film towards the penetration of electrolyte, whereas, high C_c values exhibit high water uptake tendency of the coating. On the other hand, the epoxy coatings with PPy/GA composites (PA1, PA2, PA3 and PA4) demonstrated a comparatively high R_{pore} and low C_c , signifying superior corrosion resistance in 3.5% NaCl solution (Table S5). The values of Warburg impedance is also noted to be significantly higher than the epoxy coating, throughout the immersion time of 30 days. It is interesting to mention that the epoxy coating with 2.0 wt% loading of PPy/GA composite does not evidence the diffusion controlled corrosion reaction (absence of diffusion tail in **Fig. 4** and **5**) till 20 days of immersion (Table S5). High R_{pore} values and low C_c proved the superior barrier property of the coating PA2. The coating passivates the underlying metal efficiently, even in the presence of highly diffusive chloride ions.

The corresponding Bode plots of the coatings immersed in 3.5% NaCl solution for 30 days are mentioned in **Fig. 6 a-g**. The low frequency region of the Bode plot has special significance. A high modulus of impedance ($|Z|$) in this region represents the effective barrier property of the surface coatings [68-70]. For epoxy coating, the $|Z|$ remained low throughout the immersion period. It can be noticed from **Fig. 6a-d**, that the $|Z|$ remained significantly high (till 4 days of immersion) for the epoxy coating with 1.0 wt% loading of

PPy/GA composite (PA1). However, the barrier property of this coating formulation reduced significantly after 4 days of immersion (**Fig. 6 e-g**). This could be due to the initiation of diffusion of electrolyte at the

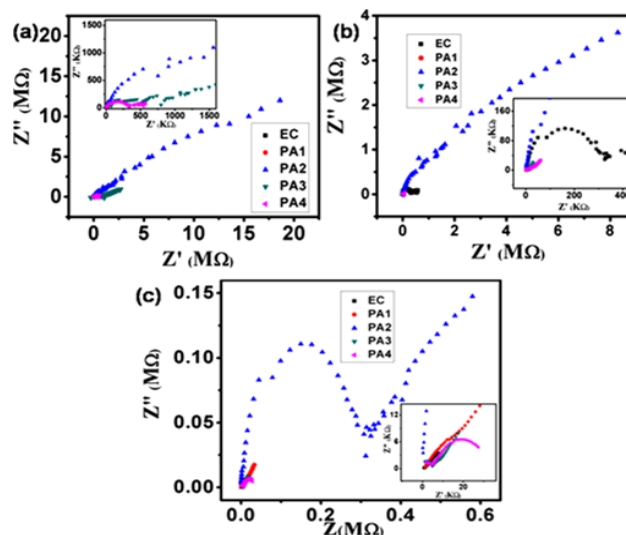


Fig. 5. Nyquist curves of epoxy coatings (EC) and epoxy coatings with 1.0 wt% (PA1), 2.0 wt% (PA2), 3.0 wt% (PA3), 4.0 wt% (PA4) loading of Polypyrrole/Gum Acacia (PPy/GA) composite after (a) 10 days, (b) 20 days and (c) 30 days of immersion in 3.5% NaCl solution at room temperature ($30 \pm 2^\circ\text{C}$).

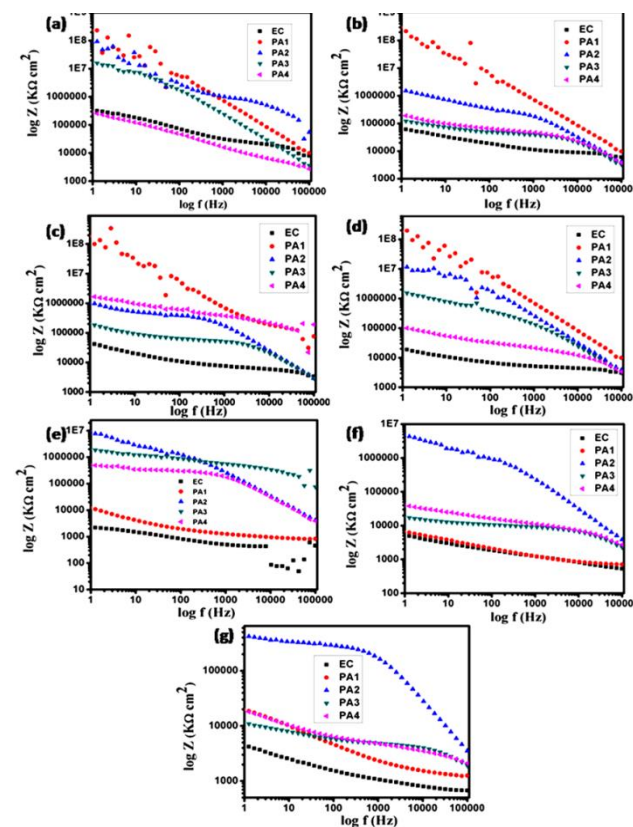


Fig. 6. Bode curves of epoxy coatings (EC) and epoxy coatings with 1.0 wt% (PA1), 2.0 wt% (PA2), 3.0 wt% (PA3), 4.0 wt% (PA4) loading of Polypyrrole/Gum Acacia (PPy/GA) composite after (a) 1/6 day, (b) 1 day, (c) 2 days, (d) 4 days, (e) 10 days (f) 20 days and (g) 30 days of immersion in 3.5% NaCl solution at room temperature ($30 \pm 2^\circ\text{C}$).

coating/electrolyte interface. Some interesting trend of Bode curves are observed for epoxy coatings with 2.0 wt% loading of PPy/GA composite (PA2). The $|Z|$ remained high in the initial hrs of immersion followed by continuous decrease in the values till 4 days of immersion. Beyond this immersion period, the modulus of impedance increased significantly and remained high till the end of immersion period (30 days).

The observation of this type of behaviour (increasing and decreasing $|Z|$ values) in a coating system gives an idea about the occurrence of competitive adsorption of electrolyte and repassivation behaviour of the surface coating. The presence of Polypyrrole and Gum Acacia in the coating helps to form protective oxide layer that passivates the freshly formed active corrosion sites on the surface of the coating. The excellent protective property of the so formed oxide layer is maintained high for longer periods of immersion. This synergy of Polypyrrole and Gum Acacia is the basic reason for the superior corrosion resistance of the composite coatings in the corrosive electrolyte like 3.5% NaCl solution.

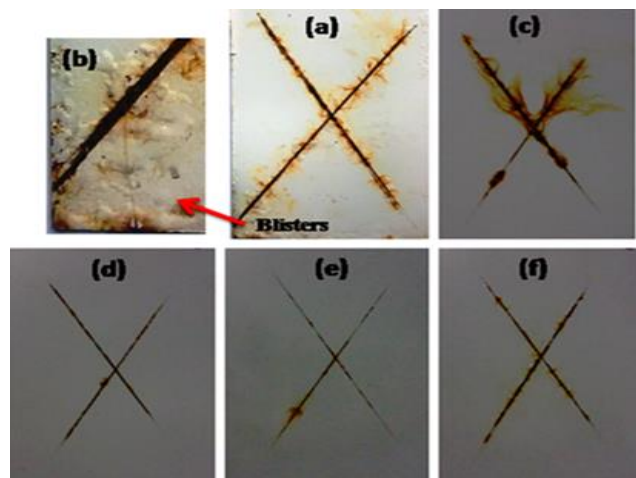


Fig. 7. Photographs of (a) epoxy coated steel panel (EC), epoxy with (c) 1.0 wt% (PA1), (d) 2.0 wt% (PA2), (e) 3.0 wt% (PA3) and (f) 4.0 wt% (PA4) loading of Polypyrrole/Gum Acacia (PPy/GA) composite after 120 days of exposure to 5.0 % NaCl in salt spray fog at room temperature (30+ 2°C). (b) Zoomed photographs of epoxy coated steel panel showing presence of blisters in the coating.

Salt spray test

Fig. 7 a-f show the salt spray test results of epoxy coating and epoxy with 1.0 wt% (PA1), 2.0 wt% (PA2), 3.0 wt% (PA3) and 4.0 wt% (PA4) loadings of PPy/GA composite coatings exposed to salt spray fog for 120 days. The epoxy coated steel panel evidenced extension of corrosion along the scribe mark (**Fig. 7a**). Additionally, severe blistering is also noticed at several regions of the coatings (**Fig. 7b**). It is well known that epoxy coatings exhibit good bonding properties with metal surface because of the polar groups present along the epoxy chain. However, ingress of corrosive ions at coating/metal interface breaks the bonding and results in the failure of these epoxy coatings. On the other hand, no blistering or extended

corrosion is noticed for epoxy with PPy/GA composite coated steel panels (**Fig. 7c-f**). PPy/GA composites present in the epoxy system act as reinforcing material in the coating. Their synergy towards corrosion inhibition enhances the overall corrosion resistance of the epoxy coating system. The composite effectively inhibit the progress of under coating corrosion and formation of oxide scale at coating/metal interface.

Conclusion

Polypyrrole/Gum Acacia (PPy/GA) composites coatings were developed on mild steel panels using powder coating technique. For this, the composites were synthesized by emulsion polymerization of pyrrole with Gum Acacia particles using suitable surfactant and oxidant. The FTIR, XRD and SEM analyses showed that the Gum Acacia particles are incorporated in the polymer matrix. The electrochemical studies (Open circuit potential, Tafel plots and Electrochemical impedance spectroscopy) exhibited that the composite coatings offered superior corrosion resistance to the metal surface for prolong immersion in 3.5% NaCl solution. The corrosion protection mechanism of the composite is explained to be due to the synergistic combination of the corrosion inhibitor properties of Gum Acacia and redox behavior of Polypyrrole. The salt spray test results also supported the electrochemical test results as the composite coatings evidenced almost no extended corrosion along the scribe mark. The reported work explains that the presence of Gum Acacia in the polymer matrix improves the corrosion resistance behavior of the coatings under extremely corrosive conditions. The PPy/GA composite coatings will be a suitable alternative for the conventional phosphate or chromate based conversion layers on mild steel substrates.

Acknowledgements

Authors thank the Director, (CSIR)-National Physical Laboratory, New Delhi for constant support and encouragement. Their thanks are extended to Mr. Brij Bisht for salt spray test results.

Author's contributions

Conceived the plan: S K D, G R; Experiments performed by: G R, P S; Data Analysis: G R, H B; Wrote paper: S K D, G R, P S, H B, H C.

Supporting information

Supporting informations are available from VBRI Press.

References

1. Fouda, A.; Mostafa, H.; Ghazy, S.; El-Farah, S; *Int. J. Electrochem. Sci.*, **2007**, 2, 182-194.
DOI: [10.1.1.510.4001](https://doi.org/10.1.1.510.4001)
2. Maayta, A. K.; Al-Rawashdeh, N. A. F.; *Corrosion Science*, **2004**, 46, 1129-1140.
DOI: [10.1016/j.corsci.2003.09.009](https://doi.org/10.1016/j.corsci.2003.09.009)
3. Al-Rawashdeh, N. A. F.; Maayta, A. K.; *Anti-Corrosion Methods and Materials.*, **2005**, 52, 160-166.
DOI: <http://dx.doi.org/10.1108/00035590510595157>
4. Shah, M. D.; Panchal, V. A.; Mudaliar, G. V.; Shah, N. K.; *Anti-Corrosion Methods and Materials.*, **2011**, 58, 125-130.
DOI: <http://dx.doi.org/10.1108/00035591111130505>

5. P. Kalenda, *Pigment & Resin Technology*, **2001**, 30, 150.
DOI: <http://dx.doi.org/10.1108/03699420110390797>
6. B. Wetzel, F. Hauptert, M. Qiu Zhang, *Composites Science and Technology*, **2003**, 63, 2055.
DOI: [http://dx.doi.org/10.1016/S0266-3538\(03\)00115-5](http://dx.doi.org/10.1016/S0266-3538(03)00115-5)
7. A. M. Atta.; N.O. Shaker.; N.E. Maysoura.; *Progress in Organic Coatings*, **2006**, 56, 100.
DOI: <http://dx.doi.org/10.1016/j.porgcoat.2005.12.004>
8. X. Shi.; T.A. Nguyen.; Z. Suo.; Y. Liu.; R. Avci.; *Surf. Coat. Technol.*, **2009**, 204, 237.
DOI: <http://dx.doi.org/10.1016/j.surfcoat.2009.06.048>
9. Mohammad Asif Alam.; El-Sayed M. Sherif.; Saeed M. Al-Zahrani.; *Int. J. Electrochem. Sci.*, **2013**, 8, 3121 – 3131.
DOI: [10.1.1.658.2466](https://doi.org/10.1.1.658.2466)
10. Nadia Hammouda.; Hacène Chadli.; Gildas Guillemot.; Kamel Belmokre.; *Advances in Chemical Engineering and Science*, **2011**, 1, 51-60.
DOI: [10.4236/aces.2011.12009](https://doi.org/10.4236/aces.2011.12009)
11. Shukla, H.S.; G.U.N.H.a.; *Journal of corrosion science and Engineering*, **2011**, 14.
DOI: <http://jcsetemp.org/jcse.org/pdf/v14preprint28.pdf>
12. Gunasekaran, G; Chauhan, L.R.; *Electrochimica Acta*, **2004**, 49, 4387-4395.
DOI: [10.1016/j.electacta.2004.04.030](https://doi.org/10.1016/j.electacta.2004.04.030)
13. Rekkab, S; H.Z; Salghi, R; Zarrouk, A; Bazzi, Lh; Hammouti, B.; Kabouche, Z.; Touzani, R.; Zougagh, M; *Journal of Material and Environment Science*, **2012**, 3, 613-627.
DOI: [10.1.1.714.4268](https://doi.org/10.1.1.714.4268)
14. Ostovari, A.; Hoseinie, S. M.; Peikari, M.; Shadizadeh, S. R.; Hashemi, S. J.; *Corrosion Science*, **2009**, 51, 1935-1949.
DOI: [10.1016/j.corsci.2009.05.024](https://doi.org/10.1016/j.corsci.2009.05.024)
15. Bothi, RAJA Pandian; R.A.A.; Hasnah, OSMAN; Khalijah, AWANG; *Acta Phys. -Chim. Sin.*, **2010**, 26, 2171-2176.
DOI: [10.3866/PKU.WHXB20100646](https://doi.org/10.3866/PKU.WHXB20100646)
16. Bothi Raja, P.; Sethuraman, M.; *Materials and Corrosion*, **2009**, 60, 22-28.
DOI: [10.1002/maco.200805027](https://doi.org/10.1002/maco.200805027)
17. Abiola, O. K.; Otaigbe, J.; Kio, O.; *Corrosion Science*, **2009**, 51, 1879-1881.
DOI: [10.1016/j.corsci.2009.04.016](https://doi.org/10.1016/j.corsci.2009.04.016)
18. Umoren, S.; Obot, I.; Ebenso, E.; Okafor, P.; Ogbobe, O.; Oguzie, E.; *Anti-Corrosion Methods and Materials*, **2006**, 53, 277-282.
DOI: <http://dx.doi.org/10.1108/00035590610692554>
19. Umoren, S. A.; *Cellulose*, **2008**, 15, 751-761.
DOI: [10.1007/s10570-008-9226-4](https://doi.org/10.1007/s10570-008-9226-4)
20. Abdallah, M.; *Portugaliae Electrochimica Acta*, **2004**, 22, 161-175.
DOI: [10.1.1.469.5881](https://doi.org/10.1.1.469.5881)
21. Umoren, S. A.; Ogbobe, O.; Igwe, I. O.; Ebenso, E. E.; *Corrosion Science*, **2008**, 50, 1998-2006.
DOI: [10.1016/j.corsci.2008.04.015](https://doi.org/10.1016/j.corsci.2008.04.015)
22. Umoren, S.; Obot, I.; Ebenso, E.; Okafor, P.; *Portugaliae Electrochimica Acta*, **2008**, 26, 267-282.
DOI: [10.1.1.626.5173](https://doi.org/10.1.1.626.5173)
23. Buchweishaija, J.; Mhinzi, G.; *Portugaliae Electrochimica Acta*, **2008**, 26, 257-265.
DOI: [10.1.1.612.5762](https://doi.org/10.1.1.612.5762)
24. Garg, U.; Tak, R.; *Journal of Chemistry*, **2010**, 7, 1220-1229.
DOI: <http://dx.doi.org/10.1155/2010/715047>
25. Sharifirad, M.; Omrani, A.; Rostami, A. A.; Khoshroo, M.; *Journal of Electroanalytical Chemistry*, **2010**, 645, 149-158.
DOI: [10.1016/j.jelechem.2010.05.005](https://doi.org/10.1016/j.jelechem.2010.05.005)
26. Yi, Y.; Liu, G.; Jin, Z.; Feng, D.; *Int. J. Electrochem. Sci*, **2013**, 8, 3540-3550.
DOI: [10.1.1.658.4568](https://doi.org/10.1.1.658.4568)
27. Gergely, A.; Pfeifer, É.; Bertóti, I.; Török, T.; Kálmán, E.; *Corrosion Science*, **2011**, 53, 3486-3499.
DOI: [10.1016/j.corsci.2011.06.014](https://doi.org/10.1016/j.corsci.2011.06.014)
28. Xu, L.; Chen, W.; Mulchandani, A.; Yan, Y.; *Angewandte Chemie International Edition*, **2005**, 44, 6009-6012.
DOI: [10.1002/anie.200500868](https://doi.org/10.1002/anie.200500868)
29. Van Schaftingen, T.; Deslouis, C.; Hubin, A.; Terryn, H.; *Electrochimica Acta*, **2006**, 51, 1695-1703.
DOI: [10.1016/j.electacta.2005.02.150](https://doi.org/10.1016/j.electacta.2005.02.150)
30. Hien, N. T. L.; Garcia, B.; Pailleret, A.; Deslouis, C.; *Electrochimica Acta*, **2005**, 50, 1747-1755.
DOI: [10.1016/j.electacta.2004.10.072](https://doi.org/10.1016/j.electacta.2004.10.072)
31. Ferreira, C. A.; Aeyach, S.; Coulaud, A.; Lacaze, P. C.; *Journal of Applied Electrochemistry*, **1999**, 29, 259-263.
DOI: [10.1023/A:1003429401453](https://doi.org/10.1023/A:1003429401453)
32. Troch-Nagels, G.; Winand, R.; Weymeersch, A.; Renard, L.; *Journal of Applied Electrochemistry*, **1992**, 22, 756-764.
DOI: [10.1007/BF01027506](https://doi.org/10.1007/BF01027506)
33. DeBerry, D. W.; *Journal of The Electrochemical Society*, **1985**, 132, 1022-1026.
DOI: [10.1149/1.2114008](https://doi.org/10.1149/1.2114008)
34. Wessling, B.; *Advanced Materials*, **1994**, 6, 226-228.
DOI: [10.1002/adma.19940060309](https://doi.org/10.1002/adma.19940060309)
35. Ruhi, G.; Bhandari, H.; Dhawan, S. K.; *Progress in Organic Coatings*, **2014**, 77, 1484-1498.
DOI: [10.1016/j.porgcoat.2014.04.013](https://doi.org/10.1016/j.porgcoat.2014.04.013)
36. Ruhi, G.; Bhandari, H.; Dhawan, S. K.; *American Journal of Polymer Science*, **2015**, 5, 18-27.
DOI: [10.5923/s.ajps.201501.03](https://doi.org/10.5923/s.ajps.201501.03)
37. Ruhi, G.; Modi, O.; Dhawan, S. K.; *Synthetic Metals* **2015**, 200, 24-39.
DOI: [10.1016/j.synthmet.2014.12.019](https://doi.org/10.1016/j.synthmet.2014.12.019)
38. A.H. El-Shazly.; A.A. Wazzan.; *Int. J. Electrochem. Sci.*, **2012**, 7, 1946 – 1957.
DOI: <http://electrochemsci.org/papers/vol7/7031946.pdf>
39. Mahmoud A. Hussein.; Salih S. Al-Juaid.; Bahaa M. Abu-Zied.; Abou-Elhagag A. Hermas.; *Int. J. Electrochem. Sci.*, **2016**, 11, 3938 - 3951
DOI: <http://www.electrochemsci.org/papers/vol11/110503938.pdf>
40. H. Ashassi-Sorkhabi.; R. Bagheri.; B. Rezaei-Moghadam.; *J. of Materi Eng and Perform* , **2016**, 25, 611–622.
DOI: [10.1007/s11665-016-1886-x](https://doi.org/10.1007/s11665-016-1886-x)
41. Toshiaki Ohtsuka.; *International Journal of Corrosion*, **2012**, 7.
DOI: [10.1155/2012/915090](https://doi.org/10.1155/2012/915090)
42. Uffana Riaz.; S.M. Ashraf.; Sharif Ahmad.; *Progress in Organic Coatings*, **2007**, 59, 138–14.
DOI: <http://dx.doi.org/10.1016/j.porgcoat.2007.02.002>
43. Denise M. Lenz a.; Michel Delamar b.; Carlos A. Ferreira a.; *Progress in Organic Coatings*, **2007**, 58, 64–69.
DOI: <http://dx.doi.org/10.1016/j.porgcoat.2006.12.002>
44. Tiwari, A.; Sen, V.; Dhakate, S.; Mishra, A.; Singh, V.; *Polymers for Advanced Technologies*, **2008**, 19, 909-914.
DOI: [10.1002/pat.1058](https://doi.org/10.1002/pat.1058)
45. Tiwari, A.; Singh, V.; *Carbohydrate Polymers*, **2008**, 74, 427-434.
DOI: [10.1016/j.carbpol.2008.03.015](https://doi.org/10.1016/j.carbpol.2008.03.015)
46. Abu-Dalo, M.; Othman, A.; Al-Rawashdeh, N.; *Int. J. Electrochem. Sci*, **2012**, 7, 9303-9324.
DOI: <http://www.electrochemsci.org/papers/vol7/71009303.pdf>
47. Almuslet, N.; Elfatih, A.; Al-Sayed, A.; Mohamed, G.; *Journal of Physical Science*, **2012**, 23, 43-53.
DOI: <http://web.usm.my/jps/23-2-12/23.2.4.pdf>
48. Radhakrishnan, S.; Sonawane, N.; Siju, C.; *Progress in Organic Coatings*, **2009**, 64, 383-386.
DOI: [10.1016/j.porgcoat.2008.07.024](https://doi.org/10.1016/j.porgcoat.2008.07.024)
49. Saravanan, K.; Sathiyarayanan, S.; Muralidharan, S.; Azim, S. S.; Venkatachari, G.; *Progress in Organic Coatings*, **2007**, 59, 160-167.
DOI: [10.1016/j.porgcoat.2007.03.002](https://doi.org/10.1016/j.porgcoat.2007.03.002)
50. Fu, Y.; Su, Y.-S.; Manthiram, A.; *Journal of The Electrochemical Society*, **2012**, 159, A1420-A1424.
DOI: [10.1149/2.027209jes](https://doi.org/10.1149/2.027209jes)
51. Lei, J.; Liang, W.; Martin, C. R.; *Synthetic Metals*, **1992**, 48, 301-312.
DOI: [10.1016/0379-6779\(92\)90233-9](https://doi.org/10.1016/0379-6779(92)90233-9)
52. Cheah, K.; Forsyth, M.; Truong, V.-T.; *Synthetic Metals*, **1998**, 94, 215-219.
DOI: [10.1016/S0379-6779\(98\)00006-X](https://doi.org/10.1016/S0379-6779(98)00006-X)
53. Sreedhar, B.; Vani, C.S.; Devi, D.K.; Rao, M.B.; Rambabu, C.; *Journal of Materials Science*, **2012**, 2, 5-13.
DOI: [10.5923/j.materials.20120201.02](https://doi.org/10.5923/j.materials.20120201.02)
54. Samui, A.; Patankar, A.; Rangarajan, J.; Deb, P.; *Progress in Organic Coatings*, **2003**, 47, 1-7.
DOI: [10.1016/S0300-9440\(02\)00117-0](https://doi.org/10.1016/S0300-9440(02)00117-0)

55. Jagtap, S. P.; Khairnar, R.; Ghatule, M. P.; International Journal of Research in Advent Technology, **2014**, 332-338.
DOI: [10.1.1.428.8455](https://doi.org/10.1.1.428.8455)
56. G. G. a. A. S. K.; Malviya, Ashwin K.; Intl. J. Surf. Engg. & Mater. Technol., **2013**, 31, 2249-7250.
57. Li, Y.; Ma, Y.; Zhang, B.; Lei, B.; Li, Y.; Acta Metallurgica Sinica (English Letters), 2014, 27, 1105-1113.
DOI: [10.1007/s40195-014-0132-5](https://doi.org/10.1007/s40195-014-0132-5)
58. Antunes, R. A.; Costa, I.; Faria, D. L. A. d.; Materials Research, **2003**, 6, 403-408.
DOI: [10.1.1.632.1367](https://doi.org/10.1.1.632.1367)
59. Bhadu, M. K.; Guin, A. K.; Singh, V.; Choudhary, S. K.; ISRN Corrosion., **2013**, 2013, 9.
DOI: [10.1155/2013/464710](https://doi.org/10.1155/2013/464710)
60. Thi Xuan Hang, T.; Truc, T. A.; Nam, T. H.; Oanh, V. K.; Jorcin, J.-B.; Pèbère, N.; Surface and Coatings Technology **2007**, 201, 7408-7415.
DOI: [10.1016/j.surfcoat.2007.02.009](https://doi.org/10.1016/j.surfcoat.2007.02.009)
61. Y. Dror.; Y. Cohen.; R. Yerushalmi-Rozen.; J. Polym. Sci., **2006**, 44, 3265-3271.
DOI: [10.1002/polb.20970](https://doi.org/10.1002/polb.20970)
62. S.A. Umoren.; I.B. Obot.; E.E. Ebenso.; N.O. Obi-Egbedi.; Int. J. Electrochem. Sci., **2008**, 3, 1029-1043.
DOI: [10.1.1.533.1438](https://doi.org/10.1.1.533.1438)
63. S.A. Umoren.; I.B. Obot.; E.E. Ebenso.; N.O. Obi-Egbedi .; R. Hookeri.; Desalination, **2009**, 247, 561-572.
DOI: [10.1016/j.desal.2008.09.005](https://doi.org/10.1016/j.desal.2008.09.005)
64. S.A. Umoren.; I.B. Obot.; E.E. Ebenso.; P.C. Okafor.; O. Ogbobe.; E.E. Oguzie.; Anti-Corrosion Methods and Materials , **2006**, 53, 277- 282.
DOI: [10.1108/00035590610692554](https://doi.org/10.1108/00035590610692554)
65. S.A. Umoren.; Cellulose ., **2008**, 15, 751-761.
DOI: [10.1007/s10570-008-9226-4](https://doi.org/10.1007/s10570-008-9226-4)
66. Pebere, N.; Picaud, T.; Duprat, M.; Dabosi, F.; Corrosion Science **1989**, 29, 1073-1086.
DOI: [10.1016/0010-938X\(89\)90045-0](https://doi.org/10.1016/0010-938X(89)90045-0)
67. J. Wang.; J. Duh.; H. Shih; Surface and Coatings Technology **1996**, 78, 248-254.
DOI: [10.1016/0257-8972\(94\)02414-6](https://doi.org/10.1016/0257-8972(94)02414-6)
68. Loveday, D.; Peterson, P.; Rodgers, B.; JCT coatings tech ., **2004**, 8, 46-52.
DOI: [10.1.1.473.9898](https://doi.org/10.1.1.473.9898)
69. Metikoš-Huković, M.; Tkalčec, E.; Kwokal, A.; Piljac, J.; Surface and Coatings Technology., **2003**, 165, 40-50.
DOI: [10.1016/S0257-8972\(02\)00732-6](https://doi.org/10.1016/S0257-8972(02)00732-6)
70. Bellucci, F.; Nicodemo, L.; Corrosion., **1993**, 49, 235-247.
DOI: [10.5006/1.3316044](https://doi.org/10.5006/1.3316044)